

PASSIVE SEISMIC ANALYSES IN THE SULTAN 7.5-MINUTE QUADRANGLE, KING AND SNOHOMISH COUNTIES, WASHINGTON

by Koichi Hayashi, Recep Cakir,
Joe D. Dragovich, Bruce A. Stoker,
Timothy J. Walsh, and Heather A. Littke

WASHINGTON
DIVISION OF GEOLOGY
AND EARTH RESOURCES

Open File Report 2013-01
October 2013

*This report has not been edited or reviewed for conformity
with Division of Geology and Earth Resources
standards or geologic nomenclature*



WASHINGTON STATE DEPARTMENT OF
Natural Resources

Peter Goldmark - Commissioner of Public Lands

PASSIVE SEISMIC ANALYSES IN THE SULTAN 7.5-MINUTE QUADRANGLE, KING AND SNOHOMISH COUNTIES, WASHINGTON

by Koichi Hayashi, Recep Cakir,
Joe D. Dragovich, Bruce A. Stoker,
Timothy J. Walsh, and Heather A. Littke

WASHINGTON
DIVISION OF GEOLOGY
AND EARTH RESOURCES

Open File Report 2013-01
October 2013

*This report has not been edited or reviewed for conformity
with Division of Geology and Earth Resources
standards or geologic nomenclature*



WASHINGTON STATE DEPARTMENT OF
Natural Resources

Peter Goldmark - Commissioner of Public Lands

DISCLAIMER

Neither the State of Washington, nor any agency thereof, nor any of their employees, makes any warranty, express or implied, or assumes any legal liability or responsibility for the accuracy, completeness, or usefulness of any information, apparatus, product, or process disclosed, or represents that its use would not infringe privately owned rights. Reference herein to any specific commercial product, process, or service by trade name, trademark, manufacturer, or otherwise, does not necessarily constitute or imply its endorsement, recommendation, or favoring by the State of Washington or any agency thereof. The views and opinions of authors expressed herein do not necessarily state or reflect those of the State of Washington or any agency thereof.

WASHINGTON STATE DEPARTMENT OF NATURAL RESOURCES

Peter Goldmark—*Commissioner of Public Lands*

DIVISION OF GEOLOGY AND EARTH RESOURCES

David K. Norman—*State Geologist*

John P. Bromley—*Assistant State Geologist*

Washington State Department of Natural Resources Division of Geology and Earth Resources

Mailing Address:

MS 47007
Olympia, WA 98504-7007

Street Address:

Natural Resources Bldg, Rm 148
1111 Washington St SE
Olympia, WA 98501

Phone: 360-902-1450

Fax: 360-902-1785

E-mail: geology@dnr.wa.gov

Website: <http://www.dnr.wa.gov/geology>

Publications List:

<http://www.dnr.wa.gov/ResearchScience/Topics/GeologyPublicationsLibrary/Pages/pubs.aspx>

Washington Geology Library Searchable Catalog:

<http://www.dnr.wa.gov/ResearchScience/Topics/GeologyPublicationsLibrary/Pages/washbib.aspx>

Washington State Geologic Information Portal:

<http://www.dnr.wa.gov/geologyportal>

Suggested Citation: Hayashi, Koichi; Cakir, Recep; Dragovich, J. D; Stoker, B. A; Walsh, T. J.; Littke, H. A., 2013, Passive seismic analyses in the Sultan 7.5-minute quadrangle, King and Snohomish Counties, Washington: Washington Division of Geology and Earth Resources Open File Report 2013-01, 9 p.

Passive Seismic Analyses in the Sultan 7.5-Minute Quadrangle, King and Snohomish Counties, Washington

by Koichi Hayashi¹, Recep Cakir², Joe D. Dragovich², Bruce A. Stoker³, Timothy J. Walsh², and Heather A. Littke²

¹ Geometrics Inc.
2190 Fortune Drive
San Jose, CA 95131

² Washington Division of
Geology and Earth Resources
MS 47007; Olympia, WA 98504-7007

³ Earth Systems
19729 207th Ave SE
Monroe, WA 98272

INTRODUCTION

Results from a simplified passive seismic (array) survey in Sultan, Washington, near the Skykomish River (Fig. 1) provide estimates for the depth to bedrock below Quaternary sedimentary deposits as a companion study to the “Geologic map of the Sultan 7.5-minute quadrangle, King and Snohomish County, Washington” (Dragovich and others, 2013). Two seismic survey sites marked Sultan B and Sultan C straddle the main strand of the Cherry Creek fault zone (CCFZ) as shown on Plate 1 of Dragovich and others (2013). Gravity, structural, subsurface and earthquake data presented by Dragovich and others (2013) suggests that the main strand of the CCFZ is a left-lateral strike-slip fault zone with a substantial eastside-up component of offset. Mapping by Dragovich and others (2013) also shows that the main strand strikes NNE and dips nearly vertically between seismic survey sites B and C (Fig. 1).

METHODS

The passive surface-wave method, or microtremor array measurements (Okada, 2003), uses ambient noise as surface waves to estimate deep S-wave velocity structure. The method is useful because it does not require an artificial wave source and the depth of investigation can easily be extended by increasing the array size. Large-scale microtremor array measurements have been widely used in Japan (Matsushima and Okada, 1990; Arai and Tokimatsu, 2005) for estimating S-wave velocity structure to a depth of several kilometers. In these measurements, data from triangle arrays with dimensions of several kilometers will constrain Rayleigh wave phase velocity in the frequency range of 0.2 to 1 Hz.

Many researchers and professionals in geophysics use the spatial autocorrelation (SPAC) method (Aki, 1957) for calculating phase velocities from ambient noise data. The method requires four (or more) sensors placed on the center and vertices of an equilateral triangle shaped array. Margaryan and others (2009) show that the SPAC method, using only two sensors (two-station microtremor array measurements or 2ST-MAM), yields phase velocities almost identical to those obtained from triangle arrays with four or seven sensors. Hayashi and Underwood (2012a, 2012b) and Hayashi and others (2013a,b) show that the 2ST-MAM method can constrain S-wave velocity profiles down to a depth of 2 to 3 km in the South Bay region of San Francisco, California, as well as in Seattle and the Olympia area, Washington.

In the present study, we surveyed two sites in the Sultan 7.5-minute quadrangle (Fig. 1) using the 2ST-MAM method. At each site, one seismograph was established at a fixed location and acquired microtremor data for the duration of the survey. A second seismograph also acquired microtremor data using variable station separations from the fixed site, with GPS-measured distances ranging from 10 to 659 m (33–2,162 ft) and 10 to 400 m (33–1,312 ft) at the B and C sites, respectively. At each measurement location, we recorded microtremor data for 10 minute to 1 hour intervals, using a 10 millisecond sample rate, for a total of several hours of data acquisition per site, increasing the record length of ambient noise with separation of seismographs. Figures 2 and 3 show the configuration of the seismographs at the two sites. To help reduce nonstationary noise, such as traffic noise, relatively quiet daytime data were acquired along roads through farm fields (Sultan survey site B) and within a park and surrounding parking lots (Sultan survey site C). McSEIS-MT Neo seismographs, three-component accelerometers manufactured by OYO Corporation, were used for data acquisition. The seismographs include GPS clocks to synchronize data.

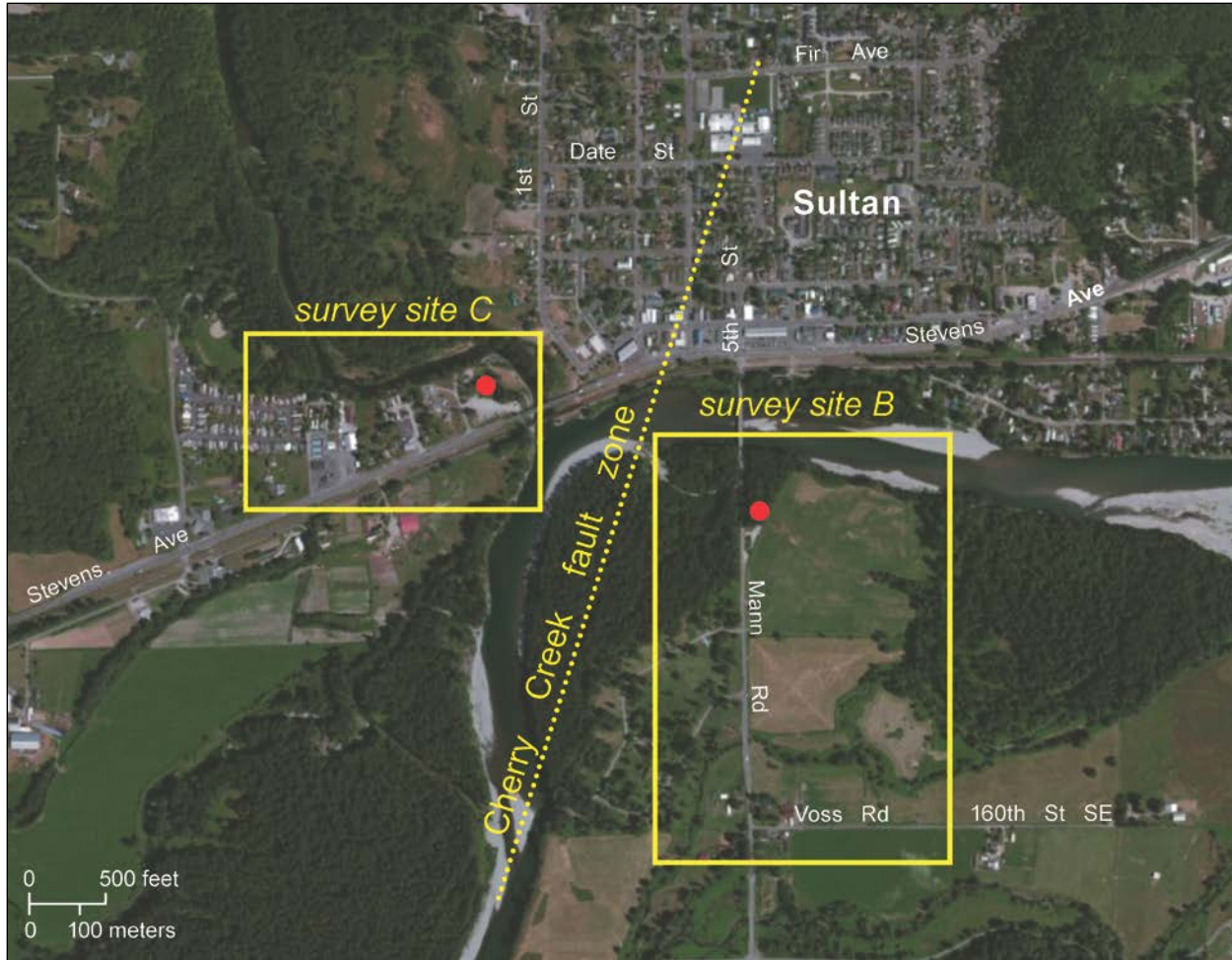


Figure 1. Location of seismic survey sites B and C. See Figs. 2 and 3 for detailed layout of each site. The concealed main strand of the Cherry Creek fault zone of Dragovich and others (2013) is shown by the yellow dotted line. The red dots indicate the starting point of the survey. The WNW–ESE-trending stratigraphic cross section and complimentary geophysical model B–B’ of Dragovich and others are directly south of this map. (Image is from http://goto.arcgisonline.com/maps/World_Imagery.)

Phase velocity processing uses the vertical component ambient noise data, which are divided into several time blocks with overlaps. Each block consists of 8,192 samples with a signal recording length of 81.92 seconds. Several blocks containing nonstationary noise signals were rejected. Coherence was calculated by each block, generating complex numbers consisting of real and imaginary parts, then the real parts of all blocks were averaged with the spatial autocorrelation (SPAC) method. The phase velocity is the velocity that minimizes the error between the SPAC coefficients and a Bessel function (first kind, zero order). Hayashi and others (2013a,b) describe details of the calculation procedure.

The inversion scheme of Suzuki and Yamanaka (2010) was applied to the observed dispersion curves, resulting in the S-wave velocity site profiles. During the inversion, the phase velocities of the dispersion curves are the observed data, with the unknown parameters being layer thickness and S-wave velocity. A genetic algorithm (Yamanaka and Ishida, 1995) was used for optimization. The search area for the inversion is based on initial velocity models created by a simple wavelength transformation in which wavelengths calculated from phase velocity and frequency pairs are divided by three to calculate corresponding depths. It is well known that the phase velocity of a Rayleigh wave is most sensitive to the depth corresponding to one-third of its wavelength, so that the wavelength divided by three implies the approximate velocity model. The weighted average of the fundamental mode and higher modes (up to the fifth mode), based on the response of the subsurface medium, generates an effective mode that we define as the theoretical phase velocity (Ikeda and others, 2012). Minimization of differences between the observed and the effective mode phase velocities is the basis for inversion.



Figure 2. Location of seismographs at Sultan survey site B. The star indicates the fixed seismograph location (latitude/ longitude: 47.858519, -121.914233). Red circles A to J indicate the moving seismograph sites. Image is http://goto.arcgisonline.com/maps/World_Imagery.

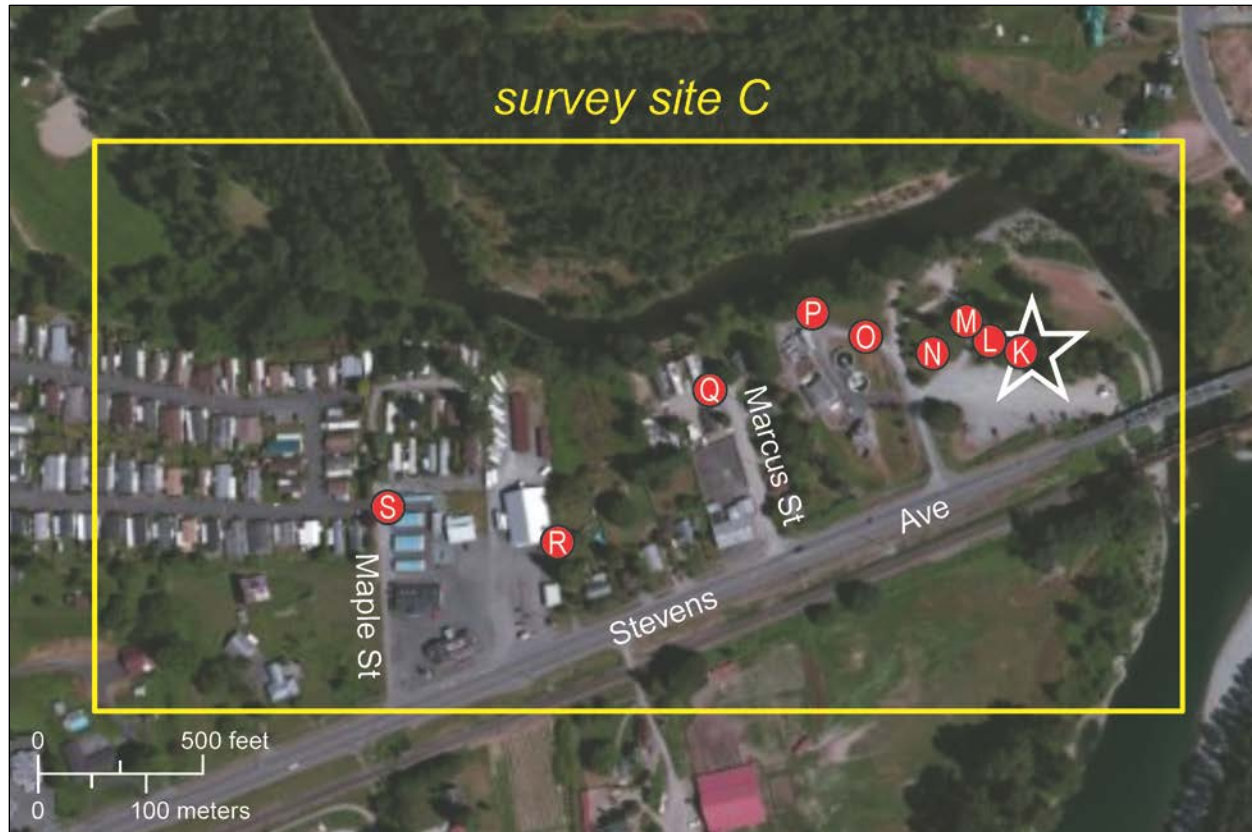


Figure 3. Location of seismographs at Sultan survey site C. The star indicates the fixed seismograph location (latitude/longitude: 47.861160, -121.822186). Red circles K to S indicate moving seismograph sites. Image is from http://goto.arcgisonline.com/maps/World_Imagery.

RESULTS

Figures 4 and 5 show comparisons of observed and theoretical phase velocities and horizontal to vertical spectral ratio (H/V) at site B. Theoretical phase velocities (effective mode) almost agree with observed velocities. The theoretical peak frequency of 0.8 Hz is generally consistent with an observed peak frequency of 0.6 Hz. Figures 6 and 7 show comparisons of observed and theoretical phase velocities and H/V at site C. Again, theoretical phase velocities (effective mode) almost agree with the observed phase velocities. A theoretical peak frequency of 0.4 Hz is generally consistent with the observed one of 0.5 Hz.

Figure 8 shows a comparison of dispersion curves. The phase velocity at site B is higher than for site C in the frequency ranges lower than 2 Hz. Site B has a peak H/V frequency of 0.6 Hz, and site C has a peak frequency of 0.5 Hz (Fig. 9). The peak frequency of 0.15 Hz at site B is due to much deeper structure. Generally speaking, shallower bedrock yields higher peak frequency and higher phase velocity in the surface wave method. The higher peak frequency of site B is consistent with the high phase velocity of the site. The difference in phase velocities and H/V data between the two sites indicates that a substantial decrease in depth to bedrock occurs between sites B and C. The data analysis implies that the approximate depth to sedimentary bedrock (defined by an S-wave velocity of 700–750 m/sec) at site B is ~150 m (~490 ft) and at site C is ~260 m (~850 ft) (Fig. 10). This is consistent with the geophysical and stratigraphic data and interpretations on stratigraphic Cross Section B–B' and geophysical Cross Section B–B' presented on the map sheet of Dragovich and others (2013). The position of this cross section is ~1,300 to 3,800 ft (396–1,158 m) south of the seismic survey sites (Fig. 1) and trends WNW–ESE, perpendicular to the CCFZ. Dragovich and others (2013) infer depths to bedrock of ~55 m (~180 ft) directly east and ~210 m (680 ft) directly west of the main strand. The bedrock depths provided in the seismic survey are consistent with these depths because the depth to bedrock increases to the north in the Skykomish valley towards the Monroe synclinal basin (Dragovich and others, 2013), and thus the depth estimates are consistent with increasing Quaternary sedimentary thickness to the north of their Cross Section B–B' in the seismic survey area.

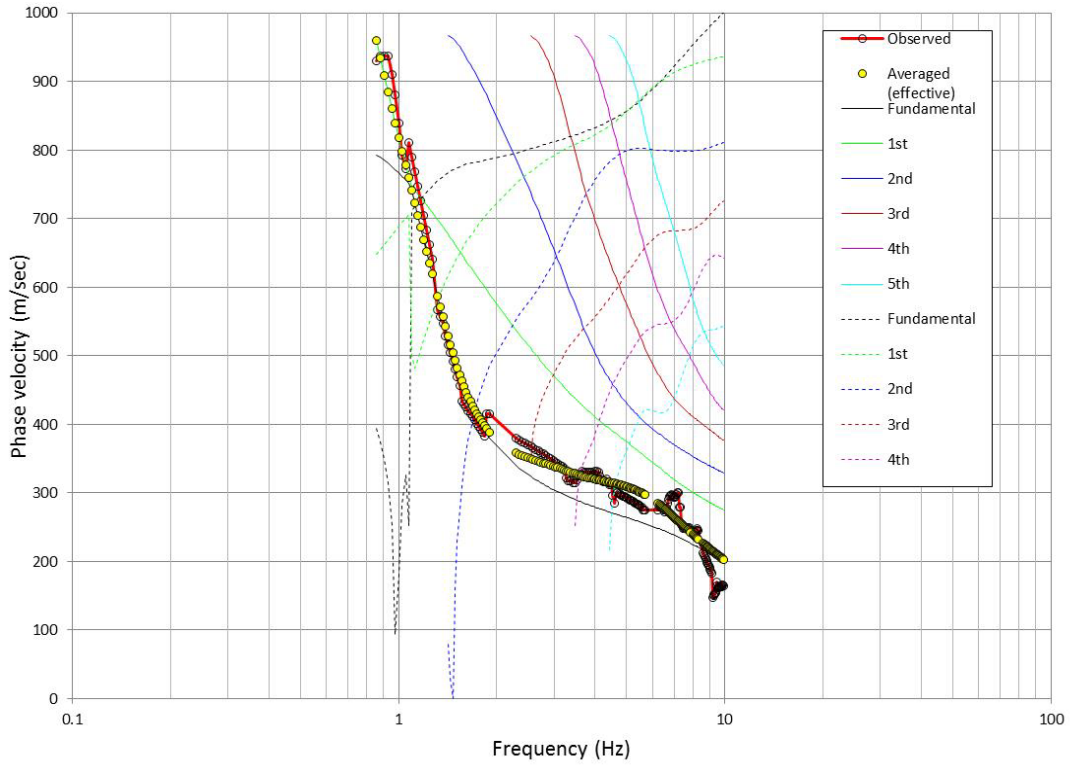


Figure 4. Comparison of observed and theoretical dispersion curves (phase velocity) for site B. Solid red line with white circles indicates observed dispersion curve. Solid and broken lines indicate fundamental and higher modes theoretical dispersion curves and their relative amplitude (response of the medium). Yellow circles indicate the effective mode of theoretical phase velocities.

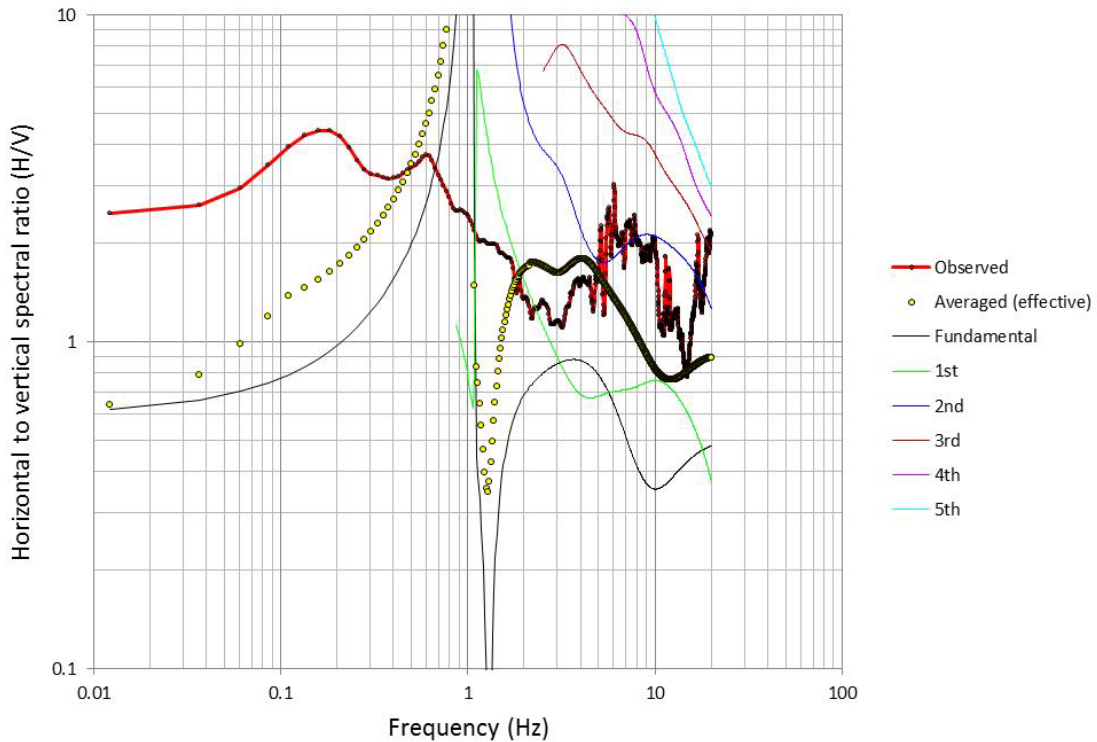


Figure 5. Comparison of observed and theoretical H/V for site B. Solid red line with black dots indicates observed H/V. Solid lines indicate theoretical H/V. Yellow circles indicate the effective mode of theoretical H/V.

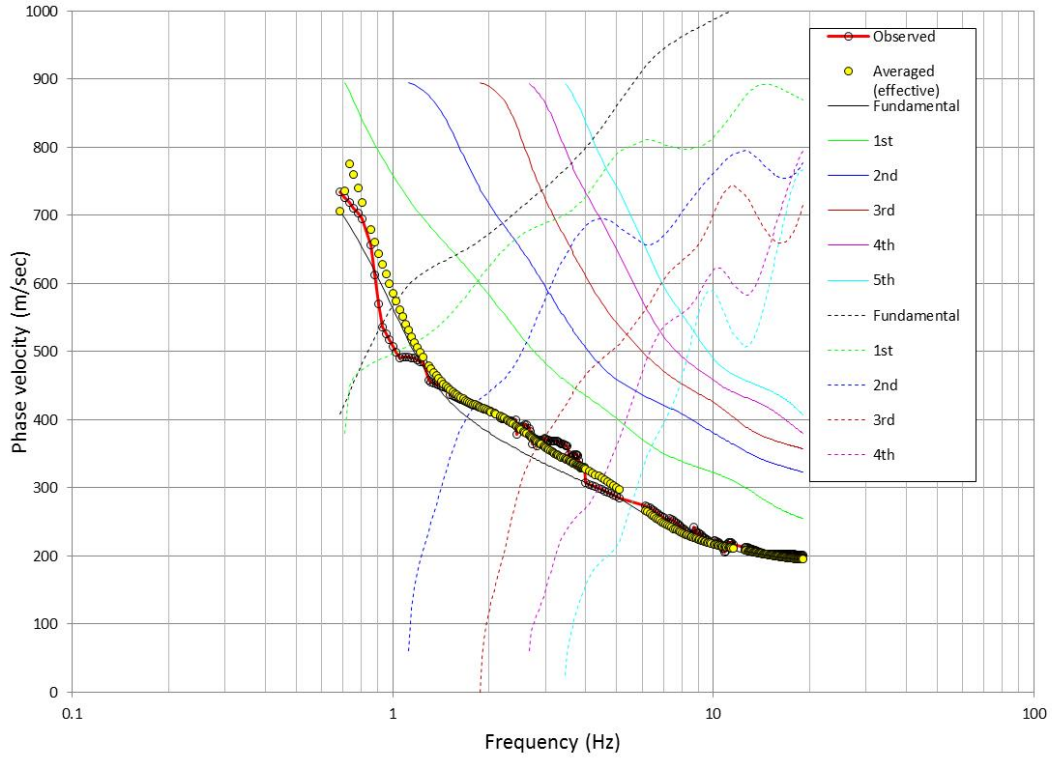


Figure 6. Comparison of observed and theoretical dispersion curves for site C. Solid red line with white circles indicates observed dispersion curve. Solid and broken lines indicate theoretical dispersion curves and their relative amplitude (response of the medium). Yellow circles indicate the effective mode of theoretical phase velocities.

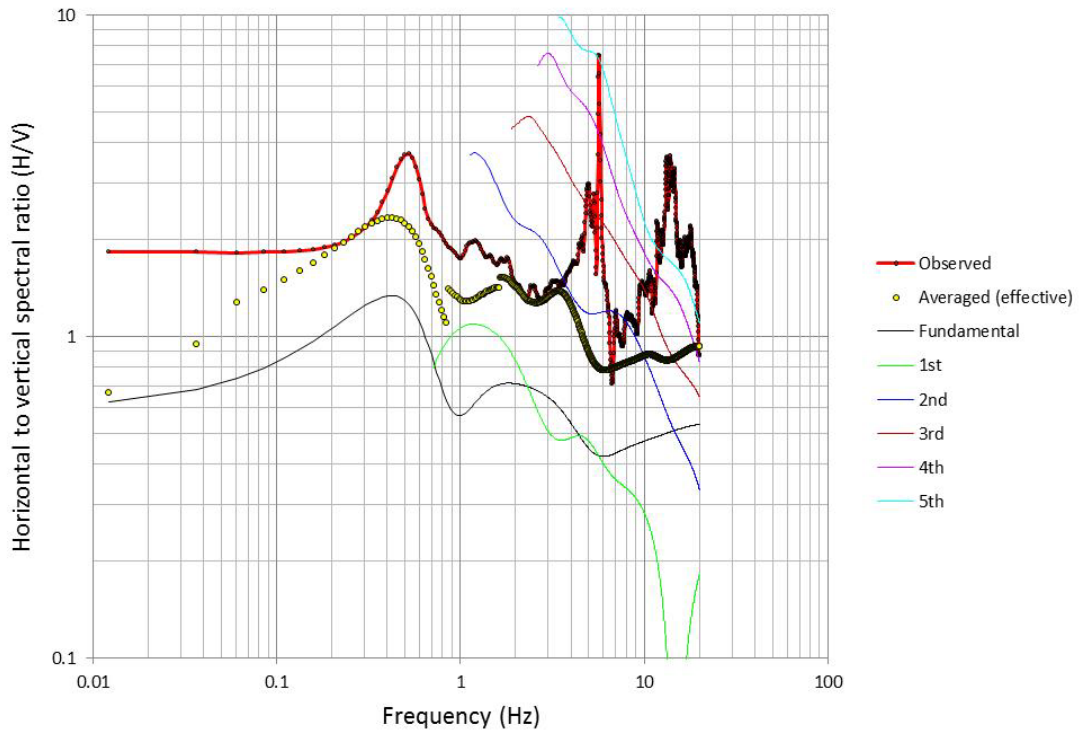


Figure 7. Comparison of observed and theoretical H/V for site C. Solid red line with black dots indicates observed H/V. Solid lines indicate theoretical H/V. Yellow circles indicate the effective mode of theoretical H/V.

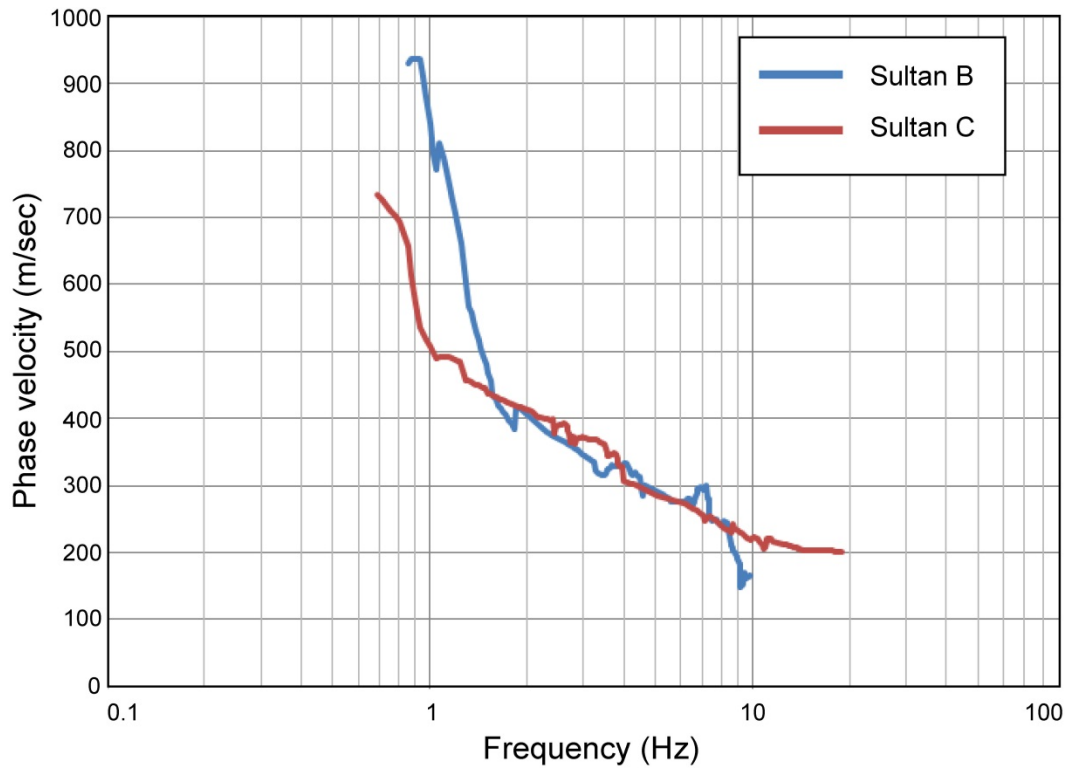


Figure 8. Comparison of phase velocity (m/s) and frequency (Hz) dispersion curves for sites B and C

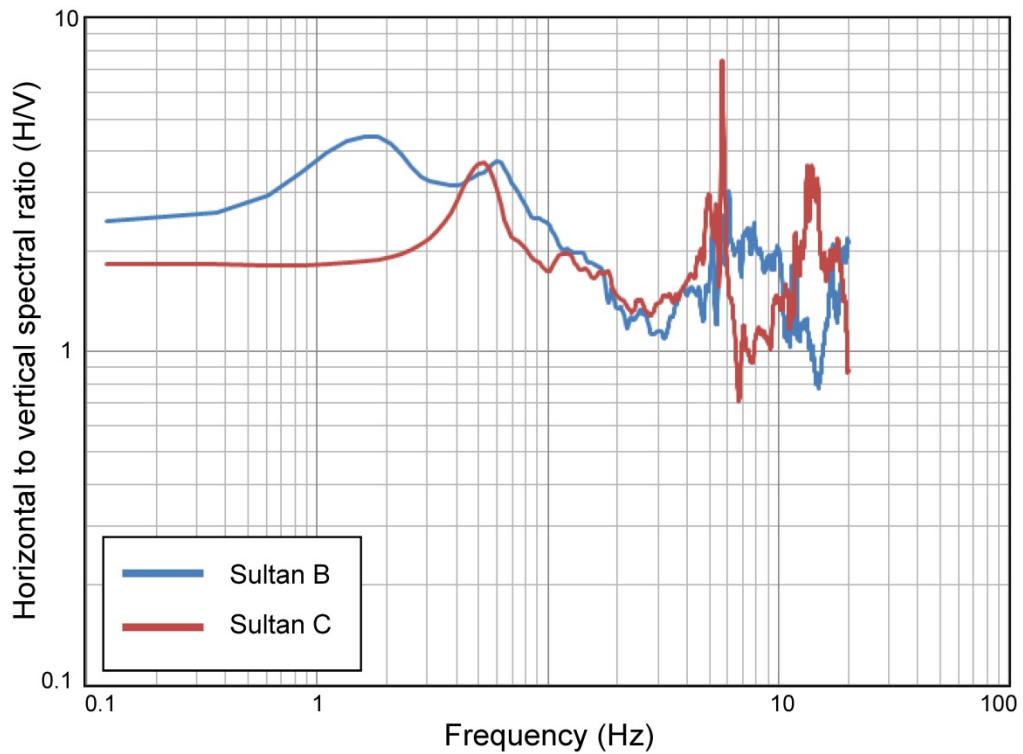


Figure 9. Comparison of H/V and frequency for sites B and C. Peak frequencies of 0.5 Hz at site B and 0.6 Hz for site C suggest bedrock is deeper at site C and thus consistent with other geophysical studies (Dragovich and others, 2013).

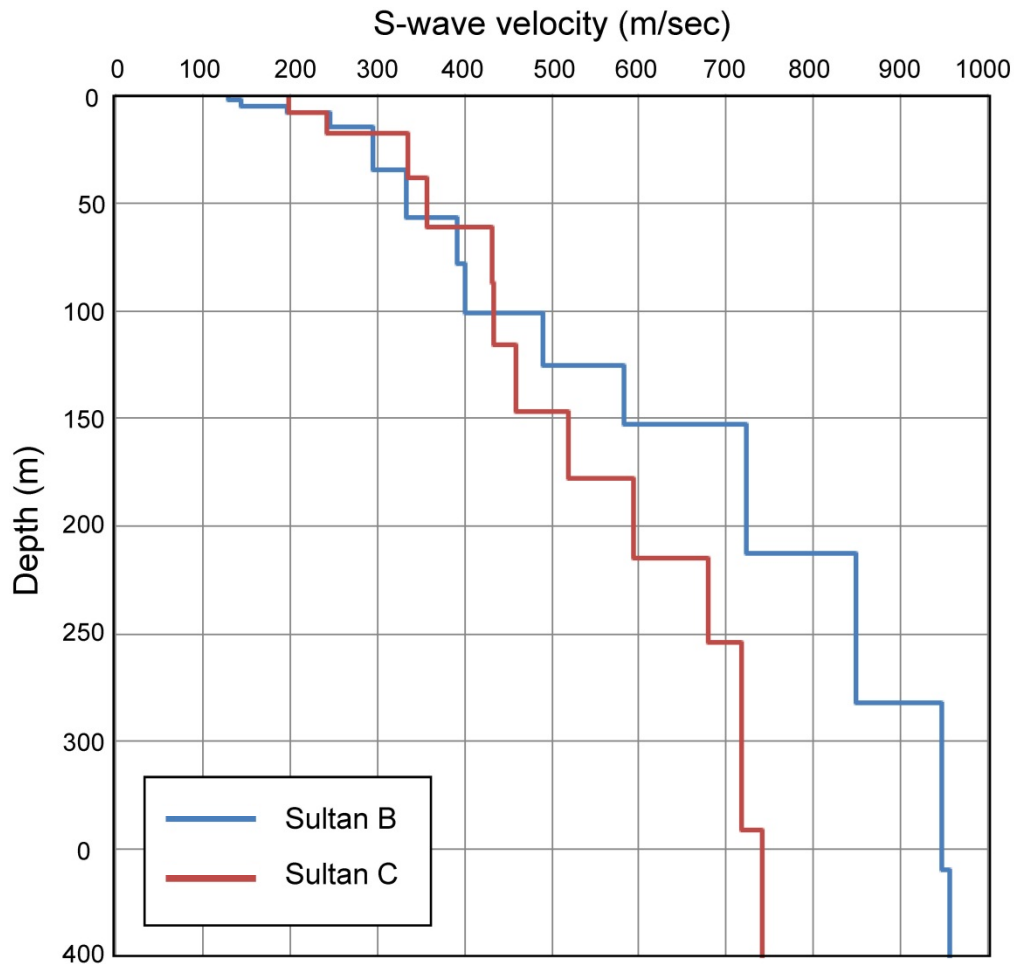


Figure 10. Comparison of inverted velocity profiles for sites B and C. The data suggests a stiff material (equivalent to sedimentary bedrock) with higher velocity (700–750 m/sec) at ~150 m (490 ft) depth for site B and with higher velocity (~700 m/sec) at ~260 m (850 ft) depth for site C, consistent with gravity and magnetic modeling and structural information indicating shallow bedrock east of the Cherry Creek fault zone main strand.

Most importantly, the seismic data confirm gravity and some well and boring data presented in Dragovich and others (2013) that indicate that the main strand of the CCFZ is spatially coincident with a distinct shallowing in bedrock in the subsurface in the Skykomish River area. The result appears to be a bedrock ridge on and east of the main strand that might be the result of Pleistocene and older oblique offset.

ACKNOWLEDGEMENTS

We thank Megan Anderson (Colorado College) for a review of the manuscript.

REFERENCES CITED

- Aki, Keiiti, 1957, Space and time spectra of stationary stochastic waves, with special reference to microtremors: Earthquake Research Institute Bulletin, v. 35, p. 415-456.
- Arai, H.; Tokimatsu, K., 2005, S-wave velocity profiling by joint inversion of microtremor dispersion curve and horizontal to vertical (H/V) spectrum: Seismological Society of America Bulletin, v. 95, p. 1766-1778.

- Dragovich, J. D.; Littke, H. A.; Mahan, S. A.; Anderson, M. L.; MacDonald, J. H., Jr.; Cakir, Recep; Stoker, B. A.; Koger, C. J.; Bethel, J. P.; DuFrane, S. A.; Smith, D. T.; Villeneuve, N. M., 2013, Geologic map of the Sultan 7.5-minute quadrangle, King and Snohomish Counties, Washington: Washington Division of Geology and Earth Resources Map Series 2013-01, 1 sheet, scale 1:24,000, with 52 p. text. [http://www.dnr.wa.gov/publications/ger_ms2013-01_geol_map_sultan_24k.zip]
- Hayashi, Koichi; Cakir, Recep; Walsh, T. J., 2013a, Using two-station microtremor array method to estimate shear-wave velocity profiles in Seattle and Olympia, Washington. *In* Proceedings of the 26th Annual Symposium on the Application of Geophysics to Engineering and Environmental Problems (SAGEEP): Environmental and Engineering Geophysical Society, 10 p. [<http://www.eegs.org/AnnualMeetingSAGEEP/SAGEEP2013/Program.aspx>]
- Hayashi, Koichi; Martin, Antony; Hatayama, Ken; Kobayashi, Takayuki, 2013b, Estimating deep S-wave velocity structure in the Los Angeles Basin using a passive surface-wave method: *The Leading Edge*, v. 32, p. 620-626.
- Hayashi, Koichi; Underwood, Deborah, 2012a, Estimating deep S-wave velocity structure using microtremor array measurements and three-component microtremor array measurements in San Francisco Bay area: Proceedings of the 25th Symposium on the Application of Geophysics to Engineering and Environmental Problems 2012 [Tucson, AZ], p. 14.
- Hayashi, Koichi; Underwood, Deborah, 2012b, Microtremor array measurements and three-component microtremor measurements in San Francisco Bay area: 15th World Conference on Earthquake Engineering [Lisbon, Portugal], p. 1634.
- Ikeda, T.; Matsuoka, T.; Tsuji, T.; Hayashi, K., 2012, Multimode inversion with amplitude response of surface waves in the spatial autocorrelation method: *Geophysics Journal Int.*, v. 190, p. 541-552
- Margaryan, S.; Yokoi, T.; Hayashi, K., 2009, Experiments on the stability of the spatial autocorrelation method (SPAC) and linear array methods and on the imaginary part of the SPAC coefficients as an indicator of data quality: *Exploration Geophysics*, v. 40, p. 121-131.
- Matsushima, T.; Okada, H., 1990, Determination of deep geological structures under urban areas using long period microtremors: *Butsuri-Tansa*, v. 43, p. 21-33.
- Okada, H., 2003, The microtremor survey method: Society of Exploration Geophysicists of Japan. Translated by Koya Suto: Geophysical Monograph Series No. 12, Society of Exploration Geophysicists, Tulsa.
- Suzuki, H.; Yamanaka H., 2010, Joint inversion using earthquake ground motion records and microtremor survey data to S-wave profile of deep sedimentary layers: *Butsuri-Tansa*, v. 63, p. 215-227 (in Japanese).
- Yamanaka, H.; Ishida, J., 1995, Phase velocity inversion using genetic algorithms: *Journal of Structural and Construction Engineering*, v. 468, p. 9-17 (in Japanese).